RSC Advances

Cite this: *RSC Advances*, 2012, **2**, 6209–6215

www.rsc.org/advances

PAPER

Bistriphenylamine-based organic sensitizers with high molar extinction coefficients for dye-sensitized solar cells

Dong Wook Chang,[a] Hoi Nok Tsao,[b] Paolo Salvatori,[c] Filippo De Angelis,[c] Michael Grätzel,[b] Su-Moon Park,[d] Liming Dai,[de] Hyo Joong Lee,*[f] Jong-Beom Baek*[d] and Mohammad K. Nazeeruddin*[b]

Received 27th April 2012, Accepted 30th April 2012
DOI: 10.1039/c2ra20798b

A series of novel bistriphenylamine-based organic sensitizers (coded as RC-dyes) with high molar extinction coefficients ($>5.0 \times 10^4$ M^{-1} cm^{-1}) have been synthesized for dye-sensitized solar cells (DSSCs). By changing the length of the π-conjugation bridge thiophene from zero to two between the donor and the acceptor part, the range of absorption and its corresponding photon-to-current conversion was modulated gradually to the low energy region in the visible spectrum. Based on the electrochemical and theoretical investigations on the electronic and geometrical structure, RC dyes were shown to be a promising candidate for efficient metal-free organic sensitizers with strong light absorption. Among RC dyes (**11**∼**13**) tested, the highest power conversion efficiency of 5.67% was obtained from **RC-13** with a short circuit current of 10.78 mA cm^{-2}, an open circuit voltage of 0.71 V, and a fill factor of 0.74 under standard AM 1.5 measurement conditions.

1. Introduction

Since being reported by Grätzel and O'Regan in 1991, dye sensitized solar cells (DSSCs) based on mesoporous metal oxide films have received great attention due to their high photon-to-current conversion efficiency, obtainable at a low fabrication cost.[1,2] With great effort by many investigators, the overall power conversion efficiency (η) of DSSCs could be improved up to about 12.5% from porphyrin dyes[2a] while metal-free organic dyes have recorded ∼10% as the best one reported so far,[2b] with advancement in knowledge of the operating mechanism and a variety of component materials.[2] As for a light-harvesting chromophore in DSSCs, various ruthenium-based sensitizers have been developed that are stable and outstandingly efficient, thus leading to a reference dye in the research of DSSCs, such as the N719 family for evaluating the performances of newly reported dyes.[3] Although the ruthenium-based sensitizers were very impressive, the metal-free organic dyes, generally composed of a donor-π-acceptor (D–π–A) configuration, have been conceived and synthesized as a promising alternative, due to their high molar absorption coefficients and convenient structural modifications, with no concern for using precious metals.[4] In this D–π–A configuration, an efficient electron transfer from donor to acceptor can happen upon photo-excitation of the sensitizer, and then the negative charges accumulated on the acceptor can be injected into the conduction band (CB) of the metal oxide. Among various kinds of functional groups tested as donors and acceptors in organic sensitizers, triphenylamine and cyanoacrylic acid have been proven to be the most promising candidates, respectively;[4] excellent electron-donating power and the aggregation-resistant nonplanar molecular configuration of triphenylamine appear to be essential for a promising donor in many organic sensitizers.[5] Cyanoacrylic acid has also been adopted as an efficient acceptor in most cases, due to its strong electron-withdrawing properties and anchoring capabilities on the TiO_2 surface. Thiophene derivatives were inserted as a π-conjugated bridge between the donor and the acceptor in most organic dyes. In attempting to make highly efficient DSSCs based on ideal organic sensitizers, one of the most important prerequisites is the design of an organic sensitizer with a high molar extinction coefficent for strong absorption of incident light.[4a] Recently, several organic sensitizers with high molar extinction coefficients have been reported as an important step toward the ideal chromophore.[6] To enhance the molar extinction coefficient of the sensitizer, it is important to choose a proper component with high absorptivity by considering a highly planar

[a]*Department of Chemical Systematic Engineering, Catholic University of Daegu, 13-13, Hayang, Gyungbuk 712-702, South Korea*
[b]*Laboratory for Photonics and Interfaces, Station 6, Institute of Chemical Sciences and Engineering, School of Basic Science, Swiss Federal Institue of Technology, CH-1015, Lausanne, Switzerland. E-mail: mdkhaja.nazeeruddin@epfl.ch; Fax: +41-21-693-4311; Tel: +41-21-693-6124*
[c]*Istituto CNR di Scienze e Tecnologie Molecalari (ISTM-CNR) and Dipartimento di Chimica, Università di Perugia, Via Elce di Sotto 8, I-06123, Perugia, Italy*
[d]*Interdisciplinary School of Green Energy/Low-Dimensional Carbon Materials Center, Ulsan National Institute of Science and Technology (UNIST), 100, Banyeon, Ulsan, 689-798, South Korea. E-mail: jbbaek@unist.ac.kr; Fax: +82-52-217-2019; Tel: +82-52-217-2510*
[e]*Department of Macromolecular Science and Engineering, Case Western Reserve University, Cleveland, Ohio 44106, USA*
[f]*Department of Chemistry, Chonbuk National University, Jeonju, 561-756, South Korea. E-mail: solarlee@jbnu.ac.kr; Fax: +82-63-270-3408; Tel: +82-63-270-3353*

molecular conformation for increased electron delocalization. Herein, a series of novel bistriphenylamine-based sensitizers, **RC-11**, **RC-12** and **RC-13** with high molar extinction coefficients (50 000 ~ 70 000) have been synthesized and then tested as a sensitizer in DSSCs. The chemical structures of sensitizers used in this study are shown in Fig. 1.

2. Experimental

2.1. Synthesis and characterization of RC-dyes

3,5-Dibromobenzaldehyde, 5-bromothiophene-2-carbaldehyde, and 5-bromo-2,2′-bithiophene-5′-carbaldehyde were obtained from TCI. Cyanoacetic acid and piperidine were used as received from Aldrich. All reagents and solvents were purchased from Aldrich. The solvents were purified by the standard method. *N*-Phenyl-*N*-(4-vinylbenzene)benzenamine (**1**) was synthesized according to the literature procedures.[7] ^{1}H and ^{13}C NMR spectra were recorded on a Varian VNMRS 600 spectrometer. UV-vis spectra were recorded on a Perkin-Elmer Lambda 900 UV-vis spectrometer, while photoluminescence emissions (PL) were measured on a Perkin-Elmer LS 55 spectrometer. Differential pulse voltammetry (DPV) measurements were performed in DMF containing 0.1 M $TBAPF_6$ and each dye (about 0.03 mM) using an EG&G 263 potentiostat/galvanostat in a three-electrode configuration. A platinum disk electrode and a platinum gauze were used as the working and the counter electrodes, respectively. A silver (Ag) wire was used as a pseudo-reference electrode with ferrocene internal standard.

3,5-Bis(4-(diphenylamino)styryl)benzaldehyde (2). **1** (5.00 g, 18.62 mmol), 3,5-dibromobenzaldehyde (2.21 g, 8.37 mmol), palladium acetate (0.11 g, 0.49 mmol), potassium carbonate (2.31 g, 16.71 mmol), and tetra-*n*-butylammoniumbromide (2.71 g, 8.37 mmol) were mixed with 20 ml dry DMF. After degassing for 30 min with Ar, the mixture was heated under Ar at 90 °C for 2 days. The resultant black mixture was diluted with chloroform and washed with 1 M HCl and brine. After drying over $MgSO_4$, the remaining liquid was concentrated and purified by column chromatography (ethyl acetate : hexane = 1 : 10) to produce 3.65 g (68%) of **3** as a yellow solid. MS (MALDI-TOF) *m*/*z* 644.19 (M^+), calcd. 644.28. Melting point 105 ~ 106 °C. ^{1}H NMR (600 MHz, acetone-d_6): δ (ppm) = 10.01 (s, 1H), 8.11 (s, 1H), 7.99 (s, 2H), 7.58 (d, 4H), 7.43 (d, 2H), 7.32–7.35 (m, 8H), 7.28 (d, 2H), 7.08–7.11 (m, 12H), 7.03 (d, 4H), ^{13}C NMR (125 MHz, acetone-d_6): δ (ppm) = 192.1, 147,8, 147.5, 139.2, 137.7, 131.2, 129.9, 129.4, 127.8, 125.6, 125.5, 124.6, 124.5, 123.4, 123.0. Anal. calcd. for $C_{47}H_{36}N_2O$: C = 87.55; H = 5.63; N = 4.34. Found: C = 87.37; H = 5.59; N = 4.22.

3-(3,5-Bis((*E*)-4-(diphenylamino)styryl)phenyl)-2-cyanoacrylic acid (RC-11). **2** (0.18 g, 0.28 mmol) and cyanoacetic acid (0.04 g, 0.47 mmol) were mixed with 5 ml acetonitrile and 5 ml chloroform. The mixture was refluxed for 5 h in the presence of piperidine (0.02 g, 0.23 mmol). After removal of the solvent, the crude product was purified by column chromatography (chloroform : methanol = 1 : 1) to produce 0.13 g (65%) **RC-11** as a deep yellow solid. MS (MALDI-TOF) *m*/*z* 711.21 (M^+), calcd. 711.29. Melting point 207 ~ 208 °C. ^{1}H NMR (600 MHz, DMSO-d_6): δ (ppm) = 8.01 (s, 1H), 7.94 (s, 2H), 7.91 (s, 1H), 7.56 (d, 4H), 7.36–7.39 (m, 8H), 7.34 (d, 2H), 7.17 (d, 2H), 7.01–7.14 (12H), 7.01 (d, 4H), ^{13}C NMR (125 MHz, DMSO-d_6): δ (ppm) = 163.5, 148.1, 147.5, 147.4, 138.8, 134.6, 131.3, 130.1, 129.6, 128.2, 126.3, 124.7, 123.8, 123.2, 119.5, 105.0. Anal. calcd. for $C_{50}H_{37}N_3O_2$: C 84.36; H = 5.24; N = 5.90. Found: C = 84.25; H = 5.17; N = 5.75.

***N*-(4-(3-(4-(Diphenylamino)styryl)-5-vinylstyryl)phenyl)-*N*-phenylbenzenamine (3).** Potassium *t*-butoxide (0.65 g, 5.80 mmol) was added to methyltriphenylphosphonium iodide (2.63 g, 5.82 mmol) solution in 15 ml dry THF. After stirring for 15 min at room temperature, **2** (2.50 g, 3.88 mmol) in 10 ml dry THF was added dropwise. The solution was further stirred at room temperature for 6 h. Finally, the solid by-product was removed by filtration and the remaining liquid was concentrated and purified by column chromatography (hexane) to produce 1.99 g (80%) of **4** as a light yellow solid. MS (MALDI-TOF) *m*/*z* 642.22 (M^+), calcd. 642.30. Melting point 75 ~ 76 °C. ^{1}H NMR (600 MHz, acetone-d_6): δ (ppm) = 7.73 (s, 1H), 7.59 (s, 2H), 7.54 (d, 4H), 7.31–7.34 (m, 8H), 7.20 (d, 4H), 7.07–7.10 (m, 12H), 7.03 (d, 4H), 6.82 (q, 1H), 5.93 (d, 1H), 5.30 (d, 1H), ^{13}C NMR (125 MHz, acetone-d_6): δ (ppm) = 147.6, 147.5, 138.4, 138.3, 136.9, 131.7, 129.4, 128.6, 127.6, 126.7, 124.5, 124.4, 123.8, 123.3, 123.2, 123.1, 113.8. Anal. calcd. for $C_{48}H_{38}N_2$: C 89.68; H = 5.96; N = 4.36. Found: C = 89.74; H = 5.82; N = 4.22.

5-(3,5-Bis(4-(diphenylamino)styryl)styryl)thiophene-2-carbaldehyde (4). **3** (0.30 g, 0.47 mmol), 5-bromothiophene-2-carbaldehyde (0.10 g, 0.52 mmol), palladium acetate (0.01 g, 0.04 mmol), potassium carbonate (0.15 g, 1.09 mmol), and tetra-*n*-butylammoniumbromide (0.17 g, 0.53 mmol) were mixed with 7 ml dry DMF. After degassing for 30 min with Ar, the mixture was heated under Ar at 90 °C for 2 days. The resultant black mixture was diluted with chloroform and washed with 1 M HCl and

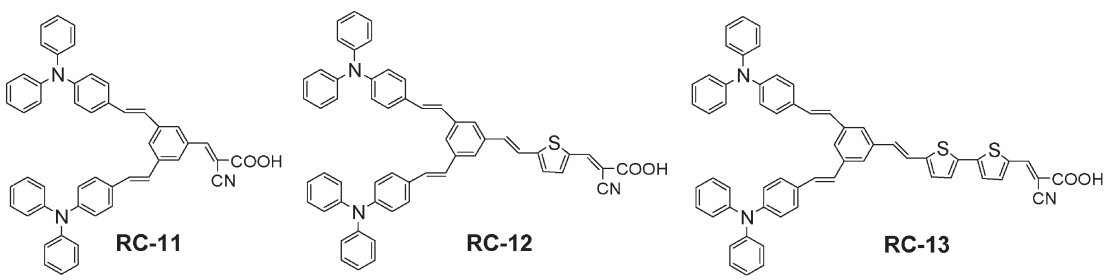

Fig. 1 Chemical structures of **RC-11**, **RC-12** and **RC-13**.

brine. After drying over $MgSO_4$, the remaining liquid was concentrated and purified by column chromatography (chloroform) to produce 0.11 g (31%) of **5** as a deep yellow solid. MS (MALDI-TOF) *m/z* 752.19 (M^+), calcd. 752.29. Melting point 118 ~ 120 °C. ^{1}H NMR (600 MHz, acetone-d_6): δ (ppm) = 9.93 (s, 1H), 7.91 (s, 1H), 7.77 (s, 2H), 7.62 (d, 1H), 7.55 (d, 4H), 7.40 (d, 1H), 7.38 (d, 1H), 7.32–7.35 (m, 9H), 7.20 (d, 4H), 7.01–7.11 (m, 12H), 7.03 (d, 4H), ^{13}C NMR (125 MHz, acetone-d_6): δ (ppm) = 183.7, 148.5, 142.9, 139.7, 138.8, 137.9, 133.3, 132.5, 130.3, 132.5, 130.3, 129.8, 128.5, 128.2, 127.3, 125.6, 125.4, 124.6, 124.2, 124.1, 122.5. Anal. calcd. for $C_{53}H_{40}N_2OS$: C 84.54; H = 5.35; N = 3.72. Found: C = 84.35; H = 5.20; N = 3.74.

(*E*)-3-(5-(3,5-Bis((*E*)-4-(diphenylamino)styryl)styryl)thiophene-2-yl)-2-cyanoacrylic acid (RC-12). 4 (0.09 g, 0.12 mmol) and cyanoacetic acid (0.03 g, 0.35 mmol) were mixed with 3 ml acetonitrile and 3 ml chloroform. The mixture was refluxed for 5 h in the presence of piperidine (0.01 g, 0.12 mmol). After removal of the solvent, the crude product was purified by column chromatography (chloroform : methanol = 1 : 1) to produce 0.07 g (72%) **RC-12** as a deep yellow solid. MS (MALDI-TOF) *m/z* 819.20 (M^+), calcd. 819.29. Melting point 278 ~ 280 °C. ^{1}H NMR (600 MHz, DMSO-d_6): δ (ppm) 8.01 (s, 1H), 7.78 (s, 2H), 7.72 (s, 1H), 7.66 (d, 1H), 7.64 (d, 1H), 7.54 (d, 4H), 7.32–7.38 (m, 10H), 7.05–7.16 (m, 16H), 6.99 (d, 4H), ^{13}C NMR (125 MHz, DMSO-d_6): δ (ppm) = 163.7, 154.1, 147.7, 147.4, 147.3, 140.7, 138.6, 137.4, 136.4, 131.6, 130.8, 130.1, 129.1, 128.1, 127.7, 126.7, 125.0, 124.7, 123.8, 123.3, 122.4, 119.7, 109.9. Anal. calcd. for $C_{56}H_{41}N_3O_2S$: C 82.02; H = 5.04; N = 5.12. Found: C = 81.89; H = 4.99; N = 5.16.

5-(5-(3,5-Bis(4-(diphenylamino)styryl)styryl)thiophene-2-yl)thiophene carbaldehyde (5). 3 (0.50 g, 0.78 mmol), 5-bromo-2,2′-bithiophene-5′-carbaldehyde (0.21 g, 0.77 mmol), palladium acetate (0.01 g, 0.04 mmol), potassium carbonate (0.22 g, 1.59 mmol), and tetra-*n*-butylammoniumbromide (0.25 g, 0.78 mmol) were mixed with 7 ml dry DMF. After degassing 30 min with Ar, the mixture was heated under Ar at 90 °C for 2 days. The resultant black mixture was diluted with chloroform and washed with 1 M HCl and brine. After drying over $MgSO_4$, the remaining liquid was concentrated and purified by column chromatography (chloroform) to produce 0.27 g (42%) of **6** as an orange solid. MS (MALDI-TOF) *m/z* 834.17 (M^+), calcd. 834.27. Melting point 109 ~ 110 °C. ^{1}H NMR (600 MHz, acetone-d_6): δ (ppm) = 9.93 (s, 1H), 7.93 (s, 1H), 7.72 (s, 2H), 7.74–7.57 (m, 5H), 7.57 (q, 2H), 7.37 (s, 1H), 7.32–7.34 (m, 8H), 7.24 (d, 1H), 7.19 (d, 4H), 7.14 (d, 1H), 7.01–7.11 (m, 12H), 7.03 (d, 4H), ^{13}C NMR (125 MHz, $CDCl_3$): δ (ppm) = 182.4, 147.6, 147.5, 147.1, 144.7, 141.6, 138.5, 137.4, 137.1, 134.5, 131.2, 129.8, 129.3, 128.9, 127.5, 127.4, 126.8, 126.4, 124.7, 124.6, 124.1, 123.4, 123.3, 123.1, 121.5. Anal. calcd. for $C_{57}H_{42}N_2OS_2$: C 81.98; H = 5.07; N = 3.35. Found: C = 81.82; H = 5.01; N = 3.29.

(*E*)-3-(5-(5-(3,5-Bis((*E*)-4-(diphenylamino)styryl)styryl)thiophene-2-yl)thiophene-2-yl)-2-cyanoacrylic acid (RC-13). 5 (0.10 g, 0.12 mmol) and cyanoacetic acid (0.03 g, 0.35 mmol) were mixed with 3 ml acetonitrile and 3 ml chloroform. The mixture was refluxed for 5 h in the presence of piperidine (0.01 g, 0.12 mmol). After removal of solvent, the crude product was purified by column chromatography (chloroform : methanol = 1 : 1) to produce 0.07 g (69%) **RC-13** as a red solid. MS (MALDI-TOF) *m/z* 901.21 (M^+), calcd. 901.28. Melting point 198 ~ 199 °C. ^{1}H NMR (600 MHz, DMSO-d_6): δ (ppm) = 8.18 (s, 1H), 7.76 (s, 2H), 7.73 (s, 1H), 7.65 (d, 1H), 7.60 (d, 4H), 7.52–7.54 (m, 2H), 7.38–7.42 (m, 10H), 7.32 (d, 1H), 7.19 (d, 2H), 7.11–7.15 (m, 14H), 7.04 (d, 4H), ^{13}C NMR (125 MHz, DMSO-d_6): δ (ppm) = 163.5, 147.4, 147.3, 143.8, 138.6, 137.6, 137.3, 134.7, 131.6, 130.1, 129.4, 129.0, 128.9, 128.1, 127.0, 126.8, 125.1, 124.7, 124.5, 123.8, 123.7, 123.4, 122.4, 119.4, 110.4. Anal. calcd. for $C_{60}H_{43}N_3O_2S_2$: C 79.88; H = 4.80; N = 4.66. Found: C = 79.65; H = 4.87; N = 4.75.

2.2. Fabrication and analyses of dye-sensitized solar cells (DSSCs)

The photo-anodes composed of nanocrystalline TiO_2 were prepared using the procedure reported previously.[8] FTO glass plates (Nippon Sheet Glass, Solar 4 mm thickness) were used as transparent conducting electrodes. After $TiCl_4$ treatment, a paste composed of 20 nm anatase TiO_2 particles for the transparent nanocrystalline layer was coated onto the FTO glass plates by screen printing. This coating–drying procedure was repeated to increase the thickness to about 9 μm. After drying the nanocrystalline TiO_2 layer, a paste for the scattering layer containing 400 nm anatase particles (CCIC, HPW-400) was deposited by two screen printings. The resulting layer was composed of a 9 μm transparent layer and a 5 μm scattering layer, the thicknesses being measured using an Alpha-step 200 surface profilometer (Tencor Instruments, San Jose, CA). The TiO_2 electrodes were gradually heated under an air flow, and then the TiO_2 electrodes were treated by $TiCl_4$ and sintered at 500 °C for 30 min. After cooling to about 80 °C, the TiO_2 electrodes were immersed in the **RC-11, RC-12 and RC-13** (in ethanol : THF = 1 : 1) solutions (0.3 mM dye and 5 mM 3a,7a-dihydroxy-5b-cholic acid, Cheno) and kept at room temperature overnight. Counter electrodes were prepared by coating with a drop of H_2PtCl_6 solution (2 mg Pt in 1 mL ethanol) on a FTO plate (TEC 15/2.2 mm thickness, Libbey-Owens-Ford Industries) and heating at 400 °C for 15 min. The dye-stained TiO_2 electrode and Pt counter electrode were assembled into a sealed sandwich-type cell by hot-pressing with a 25 μm thick transparent hot-melt film (Surlyn 1702, DuPont). An electrolyte solution (Z960: 1.0 M 1,3-dimethylimidazolium iodide, 0.030 M iodine, 0.050 M LiI, 0.10 M guanidinium thiocyanate, and 0.50 M *tert*-butylpyridine in a 15/85 (v/v) mixture of valeronitrile and acetonitrile) was prepared and injected into the inter-electrode space from the counter electrode side through a predrilled hole, which was then sealed with a Bynel sheet and a thin glass cover by heating. In order to measure the conversion efficiencies accurately, by avoiding the scattered light from the edge of the glass electrodes of the dyed-TiO_2 layer, the light-shading metal mask with an aperture was used on the DSSCs, so that the active area of DSCs was fixed at 0.16 cm^2, following the area of aperture.[9]

For photovoltaic measurements of the DSSCs, the irradiation source was a 450 W xenon light source (Osram XBO 450, USA) using a Tempax 113 solar filter. The output power of the AM 1.5 solar simulator was calibrated by using a reference Si photodiode equipped with a colored matched IR-cutoff filter (KG-3, Schott) in order to reduce the mismatch in the region of 350–750 nm between the simulated light and AM 1.5 to less than 2%. The measurement of IPCE was plotted as a function of excitation

wavelength using the incident light from a 300 W xenon lamp (ILC Technology, USA), which was focused through a Gemini-180 double monochromator (Jobin Yvon Ltd., U.K.).

2.3. Computational investigation

Calculations on the structure and the simulated spectra were performed using Density Functional Theory, DFT, and its Time-Dependent formulation, TDDFT, as implemented in the Gaussian program suite.[10] The ground state geometry for the protonated dyes were optimized in the gas phase within the B3LYP functional[11] using a 6-31G* basis set.[12] At the optimized ground state geometries, we performed TDDFT (MPW1K/6-31G*)[13] excited state calculations in the gas phase as well as in ethanol, adopting the non-equilibrium Conductor-like Polarizable Continuum Model, CPCM.[14] This computational set-up has been previously shown to adequately describe the electronic and optical properties of similar push–pull dyes.[15,16]

3. Results and discussions

3.1. Preparation of RC-dyes

The detailed procedures of the dye synthesis are shown in Scheme 1 in the experimental part; firstly, the key intermediate of compound **2** with a bistriphenylamine donor was synthesized by a Heck coupling reaction between vinyltriphenylamine and dibromobenzaldehyde in the presence of palladium acetate, tetrabutylammonium bromide, and potassium carbonate. Then, the thiophene-based linkers were introduced *via* the Heck reaction after modification of the aldehyde group to vinyl functionality, on the focal point of the donors. Thiophene derivatives have been widely used as a building block for efficient sensitizers, because of their well-known high polarizability as well as their tunable spectroscopic and electrochemical properties. For comparison, **RC-11** was prepared to have no linker part while **RC-12** and **RC-13** have monothiophene and bithiophene linkers between the donor and the acceptor, respectively. Finally, a cyanoacrylic acid moiety has been attached to the sensitizers by

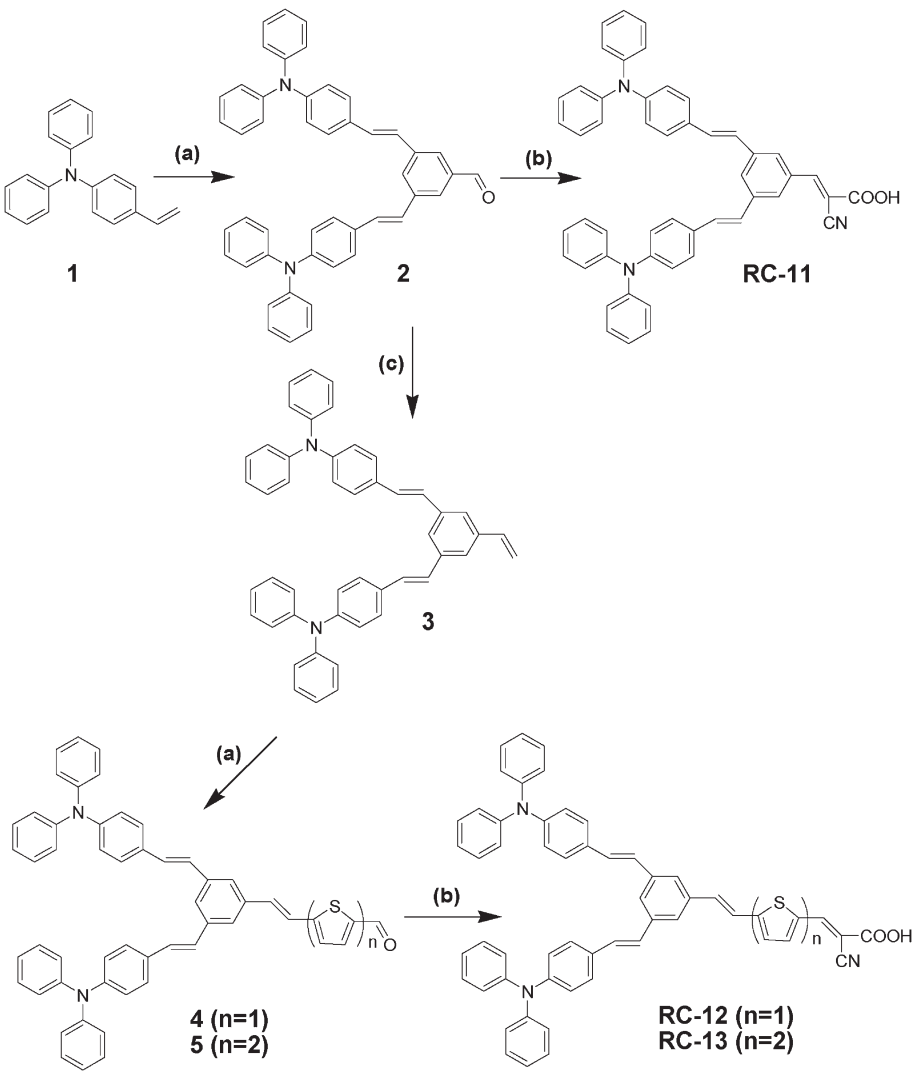

Scheme 1 Synthesis scheme of **RC-11**, **RC-12** and **RC-13**. (a) $Pd(OAc)_2$, Bu_4NBr, K_2CO_3, DMF, 90 °C, 2 days; (b) acetic acid–chloroform, reflux, 5 h; (c) methyltriphenylphosphine iodide, potassium *t*-butoxide, THF, rt, 6 h.

the Knoevenagel condensation reaction as an acceptor and anchoring group. The bistriphenylamine derivatives, **2** and **3**, can be quite useful synthetic intermediates resulting in an efficient electron-donating moiety, which can later be connected to many different types of linkers and/or acceptors through highly reactive aldehyde and vinyl functional groups on the focal points. By introducing a bulky bistriphenylamine as an electron donating component in RC-dyes, several advantages can be anticipated; stronger electron donating capability by two antennae of triphenylamine[5] and more efficient retardation of charge recombination between photoelectrons injected into the CB of TiO_2 and the oxidized form (I_3^-) of the redox couple, due to the larger steric hindrance induced by the bulky periphery of the RC-dyes.[17]

3.2. Optical and electrochemical properties of RC-dyes

Fig. 2 shows the UV-vis absorption and emission spectra of RC-sensitizers dissolved in THF. All RC-dyes show relatively high molar extinction coefficients ($\varepsilon > 50\,000\ M^{-1}\ cm^{-1}$), and the highest value was obtained for **RC-13** ($70\,900\ M^{-1}\ cm^{-1}$ at 386 nm). These optical properties of RC-sensitizers are summarized in Table 1. The optimized molecular geometries of the RC-dyes were shown to have quite a planar geometry, except for the terminal triphenylamine moiety (*vide infra*). Thus, the observed high molar extinction coefficients of RC-sensitizers probably originate from increased electron delocalization over the conjugated structures on the planar geometries and the efficient π–π* electron transitions.[6a] The electrochemical energy levels of the RC dyes were analyzed by differential pulse voltammetry (DPV) in DMF. Ag wire was used as a quasi-reference electrode with ferrocene as an internal standard. The ground-state oxidation potentials ($E_{s+/s}$) of RC dyes, corresponding to the highest occupied molecular orbital (HOMO), were measured as being located at around 1.00 V *vs.* a normal hydrogen electrode (NHE). That was more positive than the redox couple (I^-/I_3^-, ~0.35 V), ensuring that there is a sufficient driving force for dye regeneration. The zeroth–zeroth energy values of the dyes ($E_{0\text{-}0}$), which are related to the band gap energy (E_g), were estimated from the intercept of the normalized absorption and emission spectra. The lowest unoccupied molecular orbital (LUMO) level of the RC-dyes was obtained by subtracting $E_{0\text{-}0}$ from the HOMO, and was also found to be more negative than the TiO_2 conduction band (~−0.5 V *vs.* NHE) for efficient electron injection. Therefore, these new organic dyes have proper electronic energy levels as a promising sensitizer in DSSCs.

Table 1 Absorption, emission, and electrochemical properties of RC dyes

	Absorption[a]		Emission[a]		Energy level	
Dye	λ_{max}/nm	$\varepsilon/M^{-1}\ cm^{-1}$	λ_{max}/nm	$E_{0\text{-}0}$[b]/eV	$E_{s+/s}$[c]	$E_{s+/s*}$[d]
RC-11	376	50 800	483	2.93	0.96	−1.97
RC-12	384	67 500	487	2.77	1.01	−1.76
RC-13	386	70 900	520	2.58	1.03	−1.55

[a] Absorption and emission spectra were measured in THF (10^{-5} M). [b] $E_{0\text{-}0}$ was estimated from the intercept of normalized absorption and emission spectra. [c] The ground-state oxidation potential of dyes were measured in DMF by DPV. Potentials measured *vs.* Fc^+/Fc were converted to those *vs.* the normal hydrogen electrode (NHE) by addition of + 0.63 V. [d] The excited-state oxidation potential, $E_{s+/s*}$, was calculated from $E_{s+/s} - E_{0\text{-}0}$.

3.3. Theoretical investigation of RC-dyes

The optimized molecular structures of **RC-11 ~ 13** are characterized by a planar donor–acceptor arrangement, except for the terminal triphenylamine moiety, which is enforced by the conjugation occurring along the push–pull system. Thus, by extending the conjugation along the acceptor axis in the **RC-11 ~ 13** series, we expect a stabilization of the related unoccupied orbitals. A summary of the electronic structure for the considered systems is reported in Fig. 3 along with their relevant molecular orbitals.

In line with the electronic structure of related push–pull dyes,[15,16] the HOMO and HOMO − 1 of the RC dyes are in all cases localized on the donor moiety of the dye while the LUMO is delocalized over the acceptor moiety. Thus, it is expected that the efficient photo-excited electron transfer from the HOMO to the LUMO of the dyes, and then to the conduction band of TiO_2, will occur through the close position of the LUMO to the anchoring group in the excited state. The HOMO and HOMO − 1 are a degenerate couple, with contributions extending through the double donor moieties. Since the donor moiety is the same in all dyes, the HOMO energies do not show substantial variations along the series, which was also confirmed by almost the same electrochemical oxidation potentials, ~1 V (Table 1). On the other hand, the LUMOs of **RC-11 ~ 13** are in all cases delocalized over the acceptor moieties, with an increasing

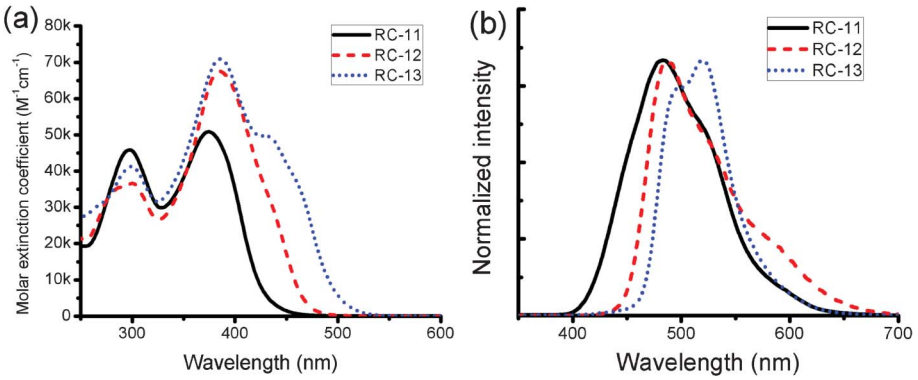

Fig. 2 (a) Absorption and (b) emission spectra of **RC-11**, **RC-12** and **RC-13** in THF. The excitation wavelength for the emission spectra was 300 nm.

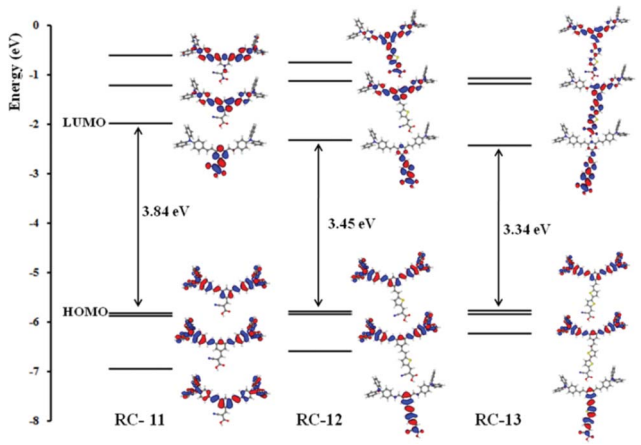

Fig. 3 Comparison between HOMO, HOMO − 1, HOMO − 2, LUMO, LUMO + 1 and LUMO + 2 molecular orbitals of the **RC-11 ~ 13** dyes in ethanol solution.

delocalization as the bridging moiety is extended from **RC-11** to **RC-13**. The LUMO energy reflects this trend, decreasing from −1.98 to −2.33 to −2.43 eV along the **RC-11 ~ 13** series.

A comparison of the calculated and experimental absorption spectra for **RC-11 ~ 13** showed a good agreement between the calculated and experimental spectra along the series, allowing us to characterize the visible absorption of the investigated compounds as essentially originating from charge transfer excitations occurring along the push–pull system of the dyes, although this is mixed with an increasing π–π* character when moving from **RC-11** to **RC-13**.

3.4. Photovoltaic properties of RC-dyes

The photovoltaic properties of RC dye-incorporated DSSCs are shown in Fig. 4 and summarized in Table 2. Under standard solar irradiation conditions of simulated AM 1.5, the **RC-13** sensitized cell exhibited the best power conversion efficiency of 5.67% with a short circuit current (J_{SC}) of 10.78 mA cm^{-2}, a open circuit voltage of 0.71 V and a fill factor (ff) of 0.74, outperforming those from **RC-11** (2.05%) and **RC-12** (3.46%). According to the current results obtained from the typical DSSCs sensitized with a series of RC dyes, the presence and length of the thiophene linker in RC dyes appear to be critical in determining the overall power conversion efficiencies in the DSSCs thereof. Without any linkage between the donor and acceptor parts, the lowest efficiency of 2.05% was obtained for **RC-11**, while the efficiencies are gradually increased from **RC-12** with a monothiophene linker to **RC-13** with a dithiophene one. Similar results have been reported before about other organic sensitizers;[18] it is believed that both broader and stronger light-absorption from sensitizers are the main reasons for this enhancement. Therefore, it is evident that a proper linker between the promising donor and acceptor unit is very critical for maximizing the capacity of the organic sensitizer composed of D–π–A. Another important factor governing the overall power conversion efficiency of RC dye-based DSSCs was observed to be that the solvent, which dissolves RC dyes, should self-assemble onto the TiO_2 surface. The different dye baths for semiconductor sensitization have a crucial effect on the performance of the DSSCs due to some reasons such as the different adsorbed amounts and binding modes of dyes anchored to the TiO_2 surface in various solvents as reported before.[19] At the current research stage, the mixed solvent of EtOH and THF (1 : 1 ratio, v/v) was found to give the best result while in each pure solvent, exhibiting a much less efficient record with RC dyes. More detailed investigations are currently under way to elucidate the effect of solvent on the behavior of the self-assembly of these bulky organic dyes and their final photovoltaic performances. To check the wavelength-dependent conversion efficiencies, the incident photon to current spectra (IPCE) from the RC dye-sensitized cells were measured (Fig. 4(b)). The IPCE spectra become more efficient in a broader range from **RC-11** *via* **RC-12** to **RC-13**, which is in accordance with their absorption

Table 2 Photovoltaic performances of DSSCs of dyes[a,b]

Dye	J_{sc}/mA cm^{-2}	V_{oc}/mV	Fill factor	η (%)
RC-11	3.38	0.79	0.77	2.05
RC-12	6.56	0.70	0.75	3.46
RC-13	10.78	0.71	0.74	5.67
N719	17.01	0.74	0.75	9.43

[a] Measured under simulated AM 1.5G conditions (100 mW cm^{-2}). [b] THF–ethanol = 1 : 1 and *t*-BuOH/ACN were used as a dye loading solvent for RC dyes and N719, respectively.

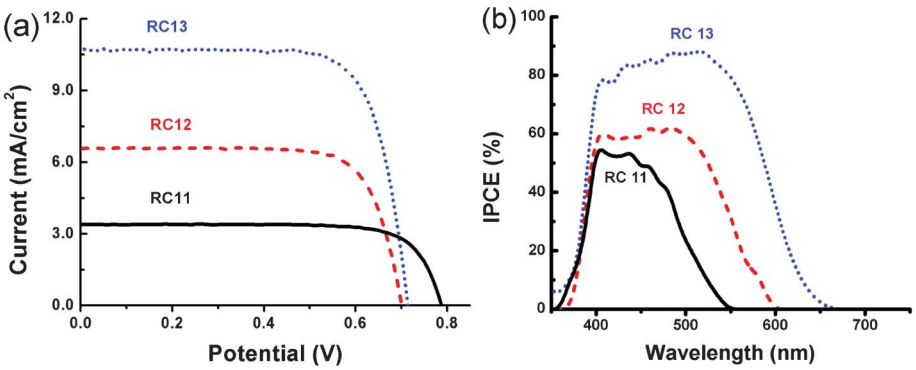

Fig. 4 (a) Photocurrent density–voltage curves of DSSCs with **RC-11**, **RC-12** and **RC-13** under AM 1.5 simulated sunlight (100 mW cm^{-2}) and (b) the IPCE action spectra of DSSCs with **RC-11**, **RC-12** and **RC-13**.

spectra (Fig. 1). In our best dye (**RC-13**), the high IPCE values (>80%) over the wide spectrum range from about 400 nm to 550 nm, with a maximum value 88% at 520 nm, were observed. This high IPCE value from the **RC-13** dye over its absorption range certifies that the current molecular configuration (bistriphenylamine-dithiophene-cyanoacrylic acid) could be a promising one for the further improvement of metal-free organic sensitizers.

4. Conclusions

A series of bistriphenylamine donor-based sensitizers (coded as RC-dyes) with high molar extinction coefficients ($5.1 \sim 7.1 \times 10^4$ M^{-1} cm^{-1}) have been synthesized based on a facile preparation route, which could easily modulate diverse structures in typical organic chromophores for applications in DSSCs. In addition to proper selection of a donor and acceptor unit, the bridging π-conjugation component was found to be crucial in designing efficient sensitizers toward an *ideal molecular converter* by strong absorption of incident light. Though the best power conversion efficiency from an **RC 13**-sensitized cell was 5.67% at the current stage, there is much room left for further enhancement by introducing some functional groups into the main structure of RC dyes and finding a more appropriate solvent to dissolve RC dyes in a favorable way for effective self-assembly onto the surface of TiO_2.

Acknowledgements

Prof. Jong-Beom Baek and Dr Mohammad K. Nazeeruddin acknowledge the financial support from the World Class University (WCU) program supported by National Research Foundation and Ministry of Education, Science and Technology of Korea. The support by the "Human Resource Development (project name: Advanced track for Si-based solar cell materials and devices, project number: 20104010100660)" of the Korea Institute of Energy Technology Evaluation and Planning (KETEP) grant funded by the Korea government Ministry of Knowledge Economy was acknowledged by H. J. Lee.

References

1 B. O'Regan and M. Grätzel, *Nature*, 1991, **353**, 737–740.
2 (*a*) A. Yella, H.-W Lee, H. N. Tsao, C. Yi, A. K. Chandiran, Md. K. Nazeeruddin, E. Wei-Guang Diau, C.-Yu Yeh, S. M. Zakeeruddin and M. Grätzel, *Science*, 2011, **334**, 629–634; (*b*) G. Zhang, H. Bala, Y. Cheng, D. Shi, X. Lv, Q. Yu and P. Wang, *Chem. Commun.*, 2009, 2198–2200.
3 (*a*) M. K. Nazeeruddin, A. Kay, I. Rodicio, R. Humphry-Baker, E. Müller, P. Liska, N. Vlachopoulos and M. Grätzel, *J. Am. Chem. Soc.*, 1993, **115**, 6382–6390; (*b*) M. K. Nazeeruddin, P. Pechy, T. Renouard, S. M. Zakeeruddin, R. Humphry-Baker, P. Comte, P. Liska, L. Cevey, E. Costa, V. Shklover, L. Spiccia, G. B. Deacon, C. A. Bignozzi and M. Grätzel, *J. Am. Chem. Soc.*, 2001, **123**, 1613–1624.
4 (*a*) A. Mishra, M. K. R. Fischer and P. Bäuerle, *Angew. Chem., Int. Ed.*, 2009, **28**, 2474–2499; (*b*) Y. Ooyama and Y. Harima, *Eur. J. Org. Chem.*, 2009, 2903–2934.
5 Z. Ning and H. Tian, *Chem. Commun.*, 2009, 5483–5495.
6 (*a*) H. Choi, I. Raabe, D. Kim, F. Teocoli, C. Kim, K. Song, J. H. Yum, J. J. Ko, M. K. Naeeruddin and M. Grätzel, *Chem.–Eur. J.*, 2010, **16**, 1193–1201; (*b*) H. Chen, H. Huang, X. Huang, J. N. Clifford, A. Forneli, E. Palomares, X. Zheng, L. Zheng, X. Wang, P. Shen, B. Zhao and S. Tan, *J. Phys. Chem. C*, 2010, **114**, 3280–3286.
7 M. Behl, E. Hattemer, M. Brehmer and R. Zentel, *Macromol. Chem. Phys.*, 2002, **203**, 503–510.
8 D. P. Hagberg, J.-H. Yum, H. J. Lee, F. De Angelis, T. Marinado, K. M. Karlsson, R. Humphry-Baker, L. Sun, A. Hagfeldt, M. Grätzel and Md. K. Nazeeruddin, *J. Am. Chem. Soc.*, 2008, **130**, 6259–6266.
9 S. Ito, Md. K. Nazeeruddin, P. Liska, P. Comte, R. Charvet, P. Pechy, M. Jirousek, A. Kay, S. M. Zakeeruddin and M. Grätzel, *Progr. Photovolt.: Res. Appl.*, 2006, **14**, 589–601.
10 Gaussian 09, Revision A.1M. J. Frisch *et al.* Gaussian, Inc.: Wallingford CT, 2009.
11 P. J. Stephens, F. J. Devlin, C. F. Chabalowski and M. J. Frisch, *J. Phys. Chem.*, 1994, **98**, 11623–11627.
12 V. A. Rassolov, J. A. Pople, M. A. Ratner and T. L. Windus, *J. Chem. Phys.*, 1998, **109**, 1223–1229.
13 B. J. Lynch, P. L. Fast, M. Harris and D. G. Truhlar, *J. Phys. Chem. A*, 2000, **104**, 4811–4815.
14 M. Cossi, N. Rega, G. Scalmani and V. Barone, *J. Comput. Chem.*, 2003, **24**, 669–681.
15 A. Abbotto, N. Manfredi, C. Marinzi, F. De Angelis, E. Mosconi, J.-H. Yum, Z. Xianxi, M. K. Nazeeruddin and M. Grätzel, *Energy Environ. Sci.*, 2009, **2**, 1094–1101.
16 M. Pastore, E. Mosconi, F. De Angelis and M. Grätzel, *J. Phys. Chem. C*, 2010, **114**, 7205–7212.
17 S. A. Haque, S. Handa, K. Peter, E. Palomares, M. Thelakkat and J. R. Durrant, *Angew. Chem., Int. Ed.*, 2005, **44**, 5740–5744.
18 (*a*) W. H. Liu, I. C. Wu, C. H. Lai, P. T. Chou, Y. T. Li, C. L. Chen, Y. Y. Hsu and Y. Chi, *Chem. Commun.*, 2008, 5152; (*b*) D. P. Hagberg, T. Marinado, K. M. Karlsson, K. Nonomura, P. Qin, G. Boschloo, T. Bricnk, A. Hägfelt and L. Sun, *J. Org. Chem.*, 2007, **72**, 9550.
19 H. Tian, X. Yang, R. Chen, R. Zhang, A. Hägfelt and L. Sun, *J. Phys. Chem. C*, 2008, **112**, 11023–11033.